

First Experiences With a Wearable Multisensor Device in a Noninvasive Continuous Glucose Monitoring Study at Home, Part II: The Investigators' View

Journal of Diabetes Science and Technology
2018, Vol. 12(3) 554–561
© 2017 Diabetes Technology Society
Reprints and permissions:
sagepub.com/journalsPermissions.nav
DOI: 10.1177/1932296817740591
journals.sagepub.com/home/dst


Mattia Zanon, PhD¹, Martin Mueller, MSc¹,
Pavel Zakharov, PhD¹, Mark S. Talary, PhD¹,
Marc Donath, PhD², Werner A. Stahel, MD³,
and Andreas Caduff, PhD¹

Abstract

Background: Extensive past work showed that noninvasive continuous glucose monitoring with a wearable multisensor device worn on the upper arm provides useful information about glucose trends to improve diabetes therapy in controlled and semicontrolled conditions.

Method: To test previous findings also in uncontrolled conditions, a long term at home study has been organized to collect multisensor and reference glucose data in a population of 20 type I diabetes subjects. A total of 1072 study days were collected and a fully on-line compatible algorithmic routine linking multisensor data to glucose applied to estimate glucose levels noninvasively.

Results: The algorithm used here calculates glucose values from sensor data and adds a constant obtained by a daily calibration. It provides point inaccuracy measured by a MARD of 35.4 mg/dL on test data. This is higher than current state-of-the-art minimally invasive devices, but still 86.9% of glucose rate points fall within the zone $A_R + B_R$.

Conclusions: The multisensor device and the algorithmic routine used earlier in controlled conditions tracks glucose changes also in uncontrolled conditions, although with lower accuracy. The examination of learning curves suggests that obtaining more data would not improve the results. Therefore, further efforts would focus on the development of more complex algorithmic routines able to compensate for environmental and physiological confounders better.

Keywords

multisensor, diabetes, T1DM, algorithm, dielectric spectroscopy

Diabetes is a widespread disease affecting 422 million people worldwide in 2014 according to a World Health Organization report.¹ It occurs when the glucose-insulin regulatory system fails to maintain glucose levels in blood within the euglycemic range of 70 ± 180 mg/dL, leading to long and short term complications. In this context, glucose sensors played a crucial role in the last years to improve diabetes management and therapy. Self-monitoring blood glucose (SMBG) sensors provided invasive and sparse glucose measures used to retrospectively analyze and adjust therapy parameters.² More recently, minimally invasive continuous glucose monitoring (CGM) sensors provided less invasive and almost continuous data, describing the dynamic of the system being measured and enabling further applications like the prediction

of hypo- and hyperglycemic alarms,³ the artificial pancreas for automatic control of glucose levels in blood,^{4,5} personalized lifestyle change suggestions to prevent long-term metabolic consequences,⁶ and others.^{7,8} Noninvasive CGM (NI-CGM) sensors are the natural next steps in the evolution of CGM devices due to obvious reasons related

¹Biovotion AG, Biovotion AG, Zurich, Switzerland

²Clinic for Endocrinology and Diabetes, University Hospital Basel, Basel, Switzerland

³Seminar for Statistics, ETH Zurich, Zurich, Switzerland

Corresponding Author:

Andreas Caduff, PhD, Biovotion AG, Kreuzstrasse 2, Zurich 8008, Switzerland.

Email: andreas.caduff@biovotion.com

to the wearer's comfort. Many noninvasive technologies were proposed over the years to measure glucose noninvasively, among others optical,⁹ electromagnetic,¹⁰ as well as acoustic¹¹ and others.¹²⁻¹⁴ These technologies provide a characterization of the biological properties of the skin or biological fluids (like saliva¹⁵ or tears¹⁶) that can be used to track glucose changes with reasonably good accuracy in strictly controlled conditions.¹⁷⁻²⁰ However, none of them provided point accuracy close to that of minimally invasive CGM devices under uncontrolled conditions. The reason being the latter measure in the sub cutis with an enzymatic sensor that is in contact with biological fluids containing glucose molecules, whereas NI-CGM devices measure skin characteristics modulated by glucose changes that are also sensitive to intrinsic (physiology related) and extrinsic (environment related) confounders. These non-glucose-related physiological confounders, like blood perfusion, sweating and orthostatic fluid shift as well as environmental ones, like temperature and humidity, must be measured and properly compensated to provide reliable and accurate glucose estimation also in uncontrolled situations typical of home use.²¹⁻²⁴ The need for such a broad characterization of phenomena lead to the development of the multisensor concept, where glucose and non-glucose-related sensors are embedded within the same device.²⁰ An algorithmic routine is then necessary to properly combine the measured channels for a robust estimation of glucose values. Mechanistic models relating multisensor channels and glucose are not yet available due to the complex nature of physiology in skin and underlying tissues and interaction among the aforementioned phenomena. For this reason, black-box statistical models were used previously.^{20,25,26} The bespoken challenges cause point accuracy of NI-CGM devices to be not yet at the same level as their minimally invasive counterpart. However, glucose rate of change has shown to be estimated with reasonably good accuracy and can be used as adjunctive information to SMBG reading to judge the risk associated with hypo- and hyperglycemic events in controlled or semiuncontrolled conditions.^{26,27}

The aim of this article is to report on the performance of algorithmic routines developed to analyze data from a long-term study with a wearable multisensor device for NI-CGM, showing how models developed for controlled and semicontrolled conditions are essentially still valid but require further effort to cope with unexpected events in the data typically met in uncontrolled conditions.

Methods

Study Population

Of the 23 subjects initially enrolled in the study who signed an informed consent agreement, 2 completed only block A (see Study Design section) and were thus excluded from the study and 1 withdrew before starting.

A total of 7 female and 13 male patients of Caucasian origin with type 1 diabetes, 38 ± 13 years (mean \pm SD), BMI 24.1 ± 3.0 kg/m², duration of diabetes 17.0 ± 13.0 years, HbA1c $7.5 \pm 0.9\%$, completed this study. The study was performed in accordance with Good Clinical Practice (GCP) and the Declaration of Helsinki.

Over the entire study there were 1072 accepted and a total of 191 excluded study days (runs) respectively, which represent 15% of all runs.

Study Design

After the screening visit, patients completed an in-clinic study day (block A) to be introduced to the device and get trained in the operation of the entire set up. Patients were then sent home and collected each a total of ten home-use days (block B). Patients returned for another three in-clinic days (block C), including two nights. While in the clinic, blood samples were taken routinely by the study personnel via an inserted venous catheter for blood glucose reference measurement using a HemoCue Glucose 201+ (HemoCue, Sweden) every 10 to 20 minutes. In parallel patients were performing regular SMBG via finger pricking and blood sampling, using a Ascensia Contour BMG (Bayer, Switzerland).

During the entire study, patients were noting down insulin dosing, activity levels or special events using a dedicated log book tool installed on the personal digital assistant (PDA).

After completion of the three in-clinic days (block C), patients returned home to perform at least another 20 study days under regular home use conditions during a period of 6-12 months (block D).

Multisensor System

The design and validation of the multisensor concept used in this study has been extensively reported previously.²⁸⁻³⁴ To characterize the biophysical properties of the skin and underlying tissues as well as the detrimental effects, the multisensor embeds a mix of dielectric spectroscopy (DS) and optical modules, as well as temperature, humidity, and sweat sensors. Finally, to measure motion effects, a 3-axes inertial sensor is implemented. Dielectric properties of the skin are investigated in the frequency range 0.1-200 MHz with three electrodes of different size to sample different penetration depths, in the 1-200 KHz range with one electrode and in the 1-3 GHz range with two additional grounded coplanar waveguides. Optical properties are measured with 2 entities of 3 LEDs, each at 3 different wavelengths: green (568 nm), red (660 nm), and infrared (798 nm).

All channels are sampled every 20 seconds and data transmitted via Bluetooth connection to a PDA and finally downloaded to a PC together with all other reference data.

Data Analysis Procedure

Figure 1 shows the block diagram of the data processing routine used to evaluate the multisensor data and the data

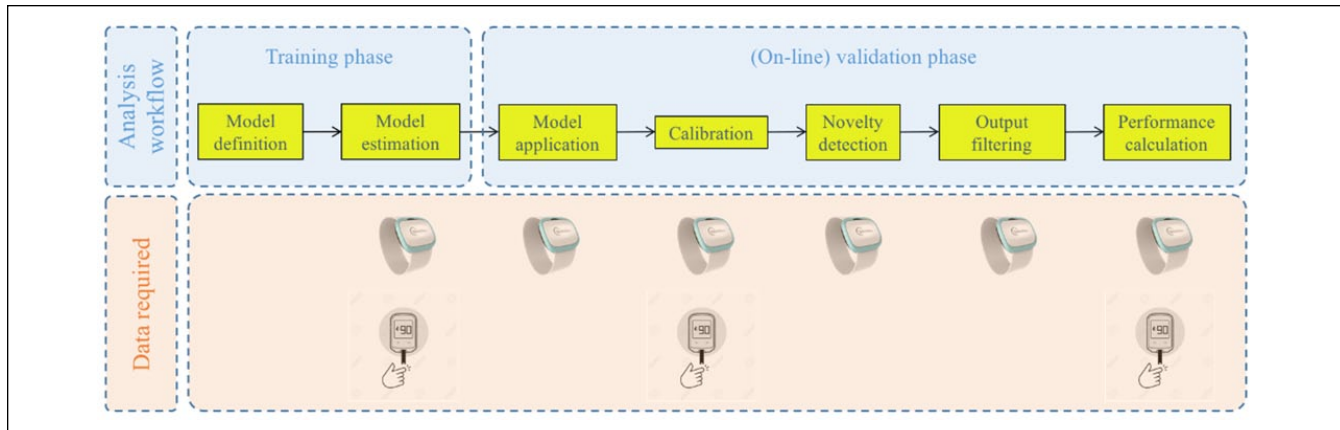


Figure 1. Block diagram of data processing and data required at each step (multisensor and reference BG).

required at each stage. The algorithm is designed to work prospectively and in real-time once it is tuned during the training phase.

Model Definition. The complex nature of the physiological system being measured and the interaction with perturbing effects support the hypothesis that measured data describe a nonlinear dynamical system, for example, the dermal blood volume variations as a function of thermoregulation.^{35,36} The internal working principles for such processes are typically expressed by mechanistic models.³⁷ However, for our problem these models have not yet been developed. We therefore use the multiple linear model:

$$y = X\beta + e \quad (1)$$

where y is a $(nx1)$ vector collecting all reference SMBG measurements, X is a $(n \times p)$ matrix containing values obtained from sensor measurements. β is the vector of p coefficients that are to be estimated from data, and e represents the portion of the glucose variation not explained by the model. The latter is assumed to be independent and identically distributed according to the normal distribution. Note that by using transformed sensor measurements and other derived terms in X , nonlinear effects and interactions can be described by the model. This structure of the model has been developed in earlier studies.^{20,25}

Model Estimation. The multisensor system used in the study is based on DS sensors that provide dielectric properties of the skin as a function of the frequency, leading in practice to a high dimensionality of the measurement space and to high correlation among subsets of variables. The problem of estimating β in (1) is then ill-conditioned and suitable techniques must be used to avoid overfitting to the training data allowing the model to generalize over unseen test data. In the past, different methodologies were used to control complexity and the best ones were those selecting only a subset of the

input variables like regularization based techniques—for example, the least absolute shrinkage and selection operator or elastic-net regression,²⁷ or greedy algorithms based on stepwise backward and/or forward selection methods.²⁵ In this work the model is derived combining a stepwise variable selection technique and the Akaike's information criterion similar to what was done in Mueller et al.²⁵

The available data from blocks A, B, C, and D are split into a training set (blocks A, B, and C) used to estimate the model and a test set (block D) to test the global model on an independent set of data not seen during the model derivation stage.³⁸

Model Application. Once the parameter vector β is estimated, glucose estimation for multisensor data at a given time instant t_i is given by a linear combination of the different j -th channels:

$$\hat{y}_i = \sum_{j=1}^p X_{i,j} \hat{\beta}_j \quad (2)$$

Calibration. Previous work showed that device calibration during the manufacturing phase causes differences among multisensor devices to be negligible.³⁹ As can be seen in Figure 2, the clustering of the DS sensor data is due to subject specific differences. To deal with these differences, an additional degree of freedom to adjust the baseline to each subject is required. Thus, a constant is added to all estimated BG values of an individual. Here, the constant is derived from a single calibration value: The first reference BG value available after the adaptation period of 75 minutes which is in the range [70, 300] mg/dL and for which the estimated glucose rate is not rapidly changing, that is, is within $-2,2$ mg/dL/min. is obtained. The constant is chosen to make the estimated BG value equal to it.⁴⁰

Novelty Detection. In uncontrolled conditions met in daily life situations unexpected events can influence the multisensor channel data and deteriorate the accuracy of glucose estimates because they were not visible in the training data and thus not

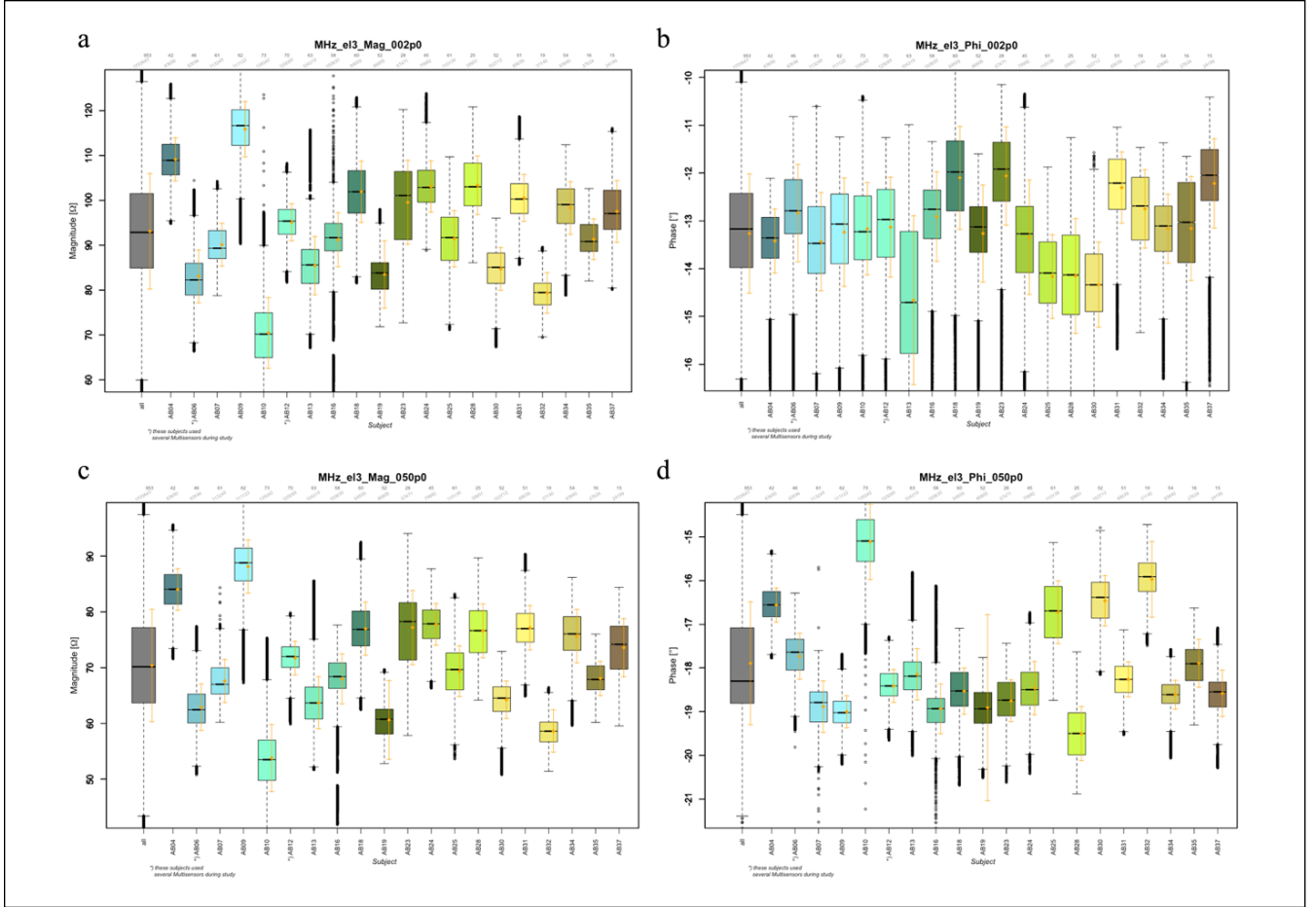


Figure 2. Boxplots of signal distribution for two channels (2 and 50 MHz, a, b and c, d respectively) measured with the long electrode and parametrized by magnitude (a, c) and phase (b, d). Mean and standard deviation are also given (orange). Given over all patients/devices (gray) and per patient/device. One device per patient, except AB06 and AB12 that used several devices.

properly compensated. The novelty detection module in cascade to the calibration stage monitors the multisensor channels and makes sure the data are within the boundaries of applicability of the model. If the module recognizes a data behavior associated with a situation it does not know how to handle properly it raises a flag, waits for 30 minutes during which glucose is not displayed, and asks for a new calibration. Describing in details the functioning of the novelty detection module is out of the scope of the present article, but we will give a brief overview. The approach consisted of training an artificial network classifier to detect situations which were manually flagged as exceptions on the basis of features describing the distribution of the data as well as from the so called innovation, that is, the difference between what the system should be doing and what is actually doing.

Output Filtering. When the estimated BG value leaves the range of 30,400 mg/dL, the estimate is suppressed for the following 30 minutes and restarted only when a new reference BG value is available for a new calibration.

Performance Calculation. Glucose values estimated by the “multisensor + algorithm routine” ensemble is compared against BG data and the accuracy measured with a set of indicators widely used in the diabetes community.

Statistical metrics. We consider the mean absolute difference (MAD), indicating how much estimated glucose values are lower or higher than the reference:

$$MAD = \frac{1}{n} \sum_{i=1}^n |y_i - \hat{y}_i| \quad (3)$$

and the mean absolute relative difference (MARD), which characterizes the relative errors (in %) of the estimated glucose:

$$MARD = \frac{1}{n} \sum_{i=1}^n \frac{|y_i - \hat{y}_i|}{y_i} \quad (4)$$

where y_i and \hat{y}_i , for $i=1, \dots, n$, are, respectively, the n reference BG samples and the glucose estimates.

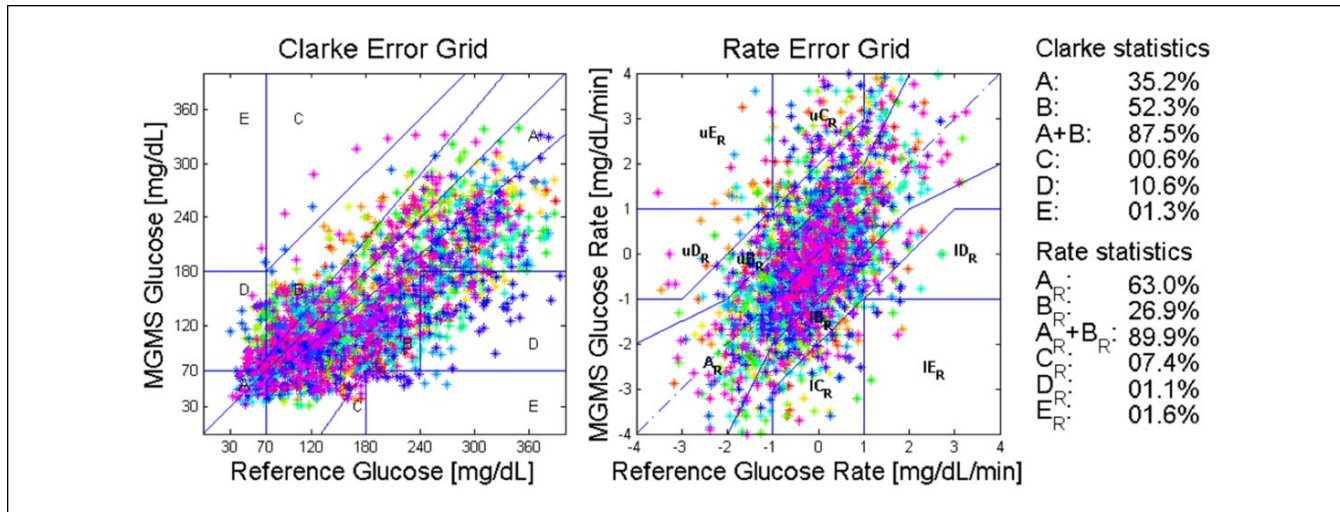


Figure 3. Internal validation results in terms of the CEG (left) and the REG (right). Colors correspond to subjects.

Table 1. Statistical Accuracy Measures for Internal Validation for the Global Model.

	Avg r^2	MAD (mg/dL)	MARD (%)	CEG A+B (A) (%)	REG A+B (A) (%)
Initial baseline adjustment	0.84	53.5	31.2	87.5 (35.2)	89.9 (63)

Metrics related to clinical relevance. Finally, a popular method used in the diabetes community to judge the point accuracy of glucose sensors is the Clarke error grid (CEG) proposed by Clarke and coworkers.⁴¹ The scatterplot of BG as estimated by the model and SMBG values is broken down into five regions labelled A to E, see Clarke et al⁴¹ for definition. The most dangerous situations are those where estimated glucose values fall into zones C/D/E because, from a clinical point of view, they will lead to unnecessary or even wrong and potentially dangerous treatments. An evolution of CEG developed for CGM sensors is the rate error grid (REG) that measures the accuracy of estimated glucose trends with analogous regions labelled from A_R to E_R; see Clarke et al⁴² for details.

Results

Internal Validation

Figure 3 and Table 1 collect the accuracy results when the global model estimated on the training data set is applied to the same data with an initial adjustment of the baseline.

External Validation

Figure 4 shows the results for the CEG and the statistics regarding the number of points falling in the different zones. The REG, measuring accuracy of estimated glucose trend, is not available because the reference sampling SMBG needed

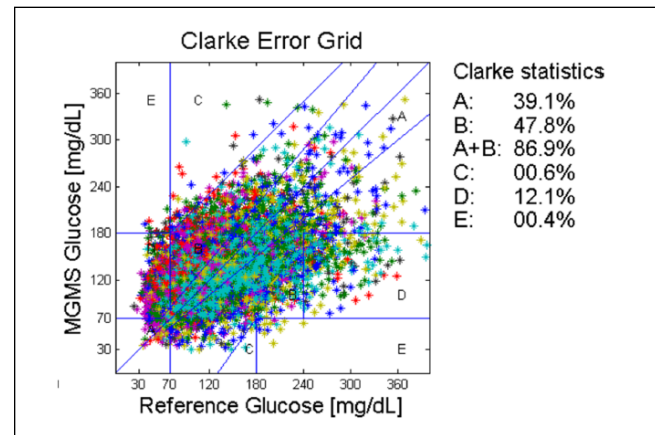


Figure 4. External validation: CEG for block D. Colors correspond to subjects.

to calculate reference trend values is too sparse since by protocol the subjects were instructed to collect 10 SMBGs during the day at home.

Table 2 reports on the results obtained after each stage of the algorithmic routine. Calibration at stable glucose levels instead of calibration after 75 min reduces the MAD of about 50%, and further improvements are achieved when monitoring multisensor channels for unexpected events and filtering the output.

Overall, the point accuracy for an externally validated, on-line compatible, global model in uncontrolled conditions

Table 2. Performance Summary for External Validation on Block D for the Global Model Estimated on Blocks A, B, and C.

	Avg r^2	MAD (mg/dL)	MARD (%)	CEG A+B (A) (%)
Initial baseline adjustment	0.50	109	107	80.7 (30.9)
+ Initial baseline adjustment at “stable” glucose	0.49	56.3	49.9	83.5 (33.0)
+ Novelty detection	0.51	52.2	46.4	84.2 (34.6)
+ Output filtering	0.50	42.1	35.4	86.9 (39.1)

Table entries show the performance improvement due to each processing routine. “Stable” glucose means SMBG rate of change within $[-2, +2]$ mg/dL/min.

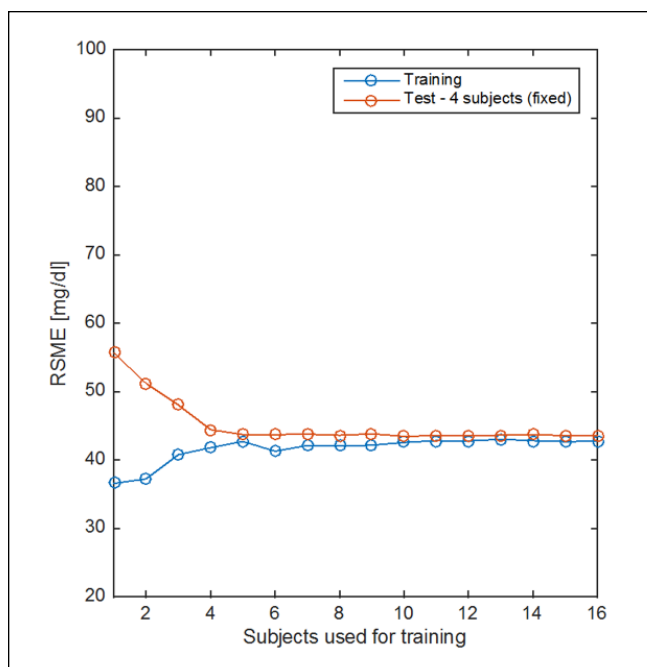


Figure 5. Learning curves for the linear model in equation 1. Train (blue) and test (red) error curves as a function of the amount of subjects' data used for training.

is lower than under controlled or semicontrolled conditions (global model MAD 29.8 mg/dL, MARD 21.1 mg/dL³⁹), likely due to perturbations not yet properly compensated.

Discussion

External validation results show that point accuracy of the NI-CGM multisensor device is not at the same level of minimally invasive ones, for example, recently showing single digit MARD value of 9%.⁴³ Understanding possible directions for improvement is essential to shrink the accuracy gap and provide a noninvasive technological solution that can be used to improve diabetes therapy. For instance, learning curves are used to analyze the bias-variance tradeoff when estimating models from data.³⁸ The bias component of the error indicates whether or not the model is complex enough to capture the complexity of the data, whereas variance of the error indicates if the model can generalize well over unseen data, that is, it is overfitting. Figure 5 shows the root mean

squared error (RMSE) used to evaluate the difference between model estimates and reference data as a function of the training data available expressed by the number of subjects included in the training set (to take into account also intersubject variability). When only few subjects are used, the training error is small because data are overfitted but the model cannot generalize on unseen data leading to big test error. As soon as the number of subjects in the training set increases the training error increases because it becomes harder to fit the data but the model will generalize better over test data (lower test error). Eventually, the train and test learning curves converge indicating the model is not overfitting anymore, that is, the model has low variance. However, train and test curves converge to RMSE value between 40–50 mg/dL indicating that the current model has a high bias and more data would not help in this case, but rather this suggests that more complex or partially adaptive models should be used to properly combine multisensor channels to account for confounding factors and intersubject variability.

Conclusions

In this work we reported some of the findings and challenges we met in a long-term study with a wearable multisensor device for NI-CGM in uncontrolled conditions at home. The goals of the study were to collect data over a long period of time, including different seasons, temperature range and climate conditions to test and to further develop the algorithms used previously in controlled and semicontrolled settings for NI-CGM. A data set of 1072 runs from T1D patients is now available including data from the multisensor as well as SMBGs and log books with meals, insulin and activity. As can be seen in Figure 2, data show the expected subject-/device-specific characteristics as in previous work.³⁹ Point accuracy is reduced in uncontrolled versus controlled conditions³⁹ and is not yet comparable to that of minimally invasive CGM but glucose rate performance in data blocks A and C as measured by the REG shows that 63% of the points are in A_R zone and almost 89.9% of the points are within zones A_R+B_R . This result opens long-term possibilities to use NI-CGM devices to applications specifically developed after the advent of CGM devices, for example, scoring of hypo- and hyperglycemic events⁴⁴ and suggestions for insulin dosing adjustments.^{45,46}

The analysis showed that the multisensor system is sensitive to glucose changes in all patients but some unexplained sources of error still persist. This can be explained with the assumptions about the model used, linear and static, that cannot capture the complexity of the measured physiological process and their interactions that are non-linear and dynamical. This is also corroborated by the learning curve analysis that suggests more data would not help. It seems that uncontrolled conditions of daily life are not yet modelled adequately. Therefore, more complicated modelling techniques could be applied to further compensate complex perturbing effects met in uncontrolled conditions. Such models might be nonlinear or adaptive in the parameters models³⁸ or better reflect knowledge of the system.^{47,48}

Abbreviations

BG, blood glucose; CEG, Clarke error grid; CGM, continuous glucose monitoring; DS, dielectric spectroscopy; MAD, mean absolute difference; MARD, mean absolute relative difference; NI-CGM, noninvasive CGM; PDA, personal digital assistant; REG, rate error grid; RMSE, root means squared error; SMBG, self-monitoring blood glucose.

Acknowledgments

Thanks to various people from former Solianis Monitoring AG and to dedicated international partners for their solid contributions that allowed expanding on the understanding of underlying mechanisms and characterization of phenomena related to noninvasive glucose monitoring.

Declaration of Conflicting Interests

The author(s) declared no potential conflicts of interest with respect to the research, authorship, and/or publication of this article.

Funding

The author(s) disclosed receipt of the following financial support for the research, authorship, and/or publication of this article: This work was supported by Solianis Monitoring AG.

References

- World Health Organization. Global report on diabetes. Geneva, Switzerland: World Health Organization. Available at: <http://www.who.int/diabetes/global-report/en/>. Accessed May 11, 2016.
- Magni P, Bellazzi R. A stochastic model to assess the variability of blood glucose time series in diabetic patients self-monitoring. *IEEE Trans Biomed Eng*. 2006;53(6):977-985.
- Sparacino G, Facchinetti A, Maran A, Cobelli C. Continuous glucose monitoring time series and hypo/hyperglycemia prevention: requirements, methods, open problems. *Curr Diabetes Rev*. 2008;4(3):181-192.
- Kovatchev B, Cheng P, Anderson SM, et al. Feasibility of long-term closed-loop control: a multicenter 6-month trial of 24/7 automated insulin delivery. *Diabetes Technol Ther*. 2017;19(1):18-24.
- Barnard KD, Wysocki T, Ullly V, et al. Closing the loop in adults, children and adolescents with suboptimally controlled type 1 diabetes under free living conditions: a psychosocial substudy [published online ahead of print April 7, 2017]. *J Diabetes Sci Technol*.
- Zeevi D, Korem T, Zmora N, et al. Personalized nutrition by prediction of glycemic responses. *Cell*. 2015;163(5):1079-1094.
- Scheiner G. CGM retrospective data analysis. *Diabetes Technol Ther*. 2016;18(Suppl. 2):S214-S222.
- Beck RW, Calhoun P, Kollman C. Use of continuous glucose monitoring as an outcome measure in clinical trials. *Diabetes Technol Ther*. 2012;14:877-882.
- Pandey R, Paidi SK, Valdez TA, et al. Noninvasive monitoring of blood glucose with Raman spectroscopy. *Acc Chem Res*. 2017;50(2):264-272.
- Levy E, Barshtein G, Livshits L, Ishai PB, Feldman Y. Dielectric response of cytoplasmic water and its connection to the vitality of human red blood cells: I. Glucose concentration influence. *J Phys Chem B*. 2016;120(39):10214-10220.
- Tachibana K, Okada K, Kobayashi R, Ishihara Y. Development of a high-sensitivity and portable cell using Helmholtz resonance for noninvasive blood glucose-level measurement based on photoacoustic spectroscopy. *Conf Proc IEEE Eng Med Biol Soc*. 2016;2016:6477-6480.
- Chen C, Zhao XL, Li ZH, Zhu ZG, Qian SH, Flewitt AJ. Current and emerging technology for continuous glucose monitoring. *Sensors (Basel)*. 2017;17(1). pii:E182.
- Vashist SK. Continuous glucose monitoring systems: a review. *Diagnostics (Basel)*. 2013;3(4):385-412.
- Hertzberg O, Bauer A, Küderle A, Pleitez MA, Mäntele W. Depth-selective photothermal IR spectroscopy of skin: potential application for non-invasive glucose measurement. *Analyst*. 2017;142(3):495-502.
- Naing C, Mak JW. Salivary glucose in monitoring glycaemia in patients with type 1 diabetes mellitus: a systematic review. *J Diabetes Metab Disord*. 2017;16:2.
- Francisco JA, Valentin H. Noninvasive continuous monitoring of tear glucose using glucose-sensing contact lenses. *Optom Vis Sci*. 2016;93(4):426-434.
- Larin KV, Eledrisi MS, Motamedi M, Esenaliev RO. Noninvasive blood glucose monitoring with optical coherence tomography: a pilot study in human subjects. *Diabetes Care*. 2002;25(12):2263-2267.
- Arnold MA, Small GW. Perspectives in analytical chemistry: noninvasive glucose sensing. *Anal Chem*. 2005;77(17):5429-5439.
- Caduff A, Dewarrat F, Talary MS, Stalder G, Heinemann L, Feldman Yu. Non-invasive glucose monitoring in patients with diabetes: a novel system based on impedance spectroscopy. *Biosens Bioelectron*. 2006;22(5):598-604.
- Caduff A, Mueller M, Megej A, et al. Characteristics of a multisensor system for non invasive glucose monitoring with external validation and prospective evaluation. *Biosens Bioelectron*. 2011;26(9):3794-3800.
- Caduff A, Talary MS, Zakharov P. Cutaneous blood perfusion as a perturbing factor for noninvasive glucose monitoring. *Diabetes Technol Ther*. 2010;12(1):1-9.
- Zakharov P, Dewarrat F, Caduff A, Talary MS. The effect of blood content on the optical and dielectric skin properties. *Physiol Meas*. 2011;32(1):131-149.

23. Harman-Boehm I, Gal A, Raykhman AM, Naidis E, Mayzel Y. Noninvasive glucose monitoring: increasing accuracy by combination of multi-technology and multi-sensors. *J Diabetes Sci Technol*. 2010;4(3):583-595.
24. Amaral CF, Brischwein M, Wolf B. Multiparameter techniques for non-invasive measurement of blood glucose. *Sensors and Actuators B-Chem*. 2009;140(1):12-16.
25. Mueller M, Talary M, Falco L, Stahel W, Caduff A. Data processing for non-invasive continuous glucose monitoring with a multi-sensor device. *J Diabetes Sci Technol*. 2011;5(3):703-713.
26. Zanon M, Sparacino G, Facchinetti A, et al. Non-invasive continuous glucose monitoring: improved accuracy of point and trend estimates of the multisensor system. *Med Biol Eng Comput*. 2012;50(10):1047-1057.
27. Zanon M, Sparacino G, Facchinetti A, Talary MS, Caduff A, Cobelli C. Regularised model identification improves accuracy of multisensor systems for noninvasive continuous glucose monitoring in diabetes management. *J Applied Mathematics*. 2013;2013:793869.
28. Caduff A, Livshits L, Hayashi Y, Feldman Yu. Cell membrane response on d-glucose studied by dielectric spectroscopy. Erythrocyte and ghost suspensions. *J Phys Chem B*. 2004;108:13827-13830.
29. Lev D, Puzenko A, Manevitch A, et al. D-glucose-induced second harmonic generation response in human erythrocytes. *J Phys Chem B*. 2009;113(8):2513-2518.
30. Livshits L, Caduff A, Talary MS, et al. The role of GLUT1 in the sugar induced dielectric response of human erythrocyte membranes. *J Phys Chem B*. 2009;113(7):2212-2220.
31. Di Biasio A, Cametti C. D-glucose-induced alterations in the electrical parameters of human erythrocyte cell membrane. *Bioelectrochemistry*. 2010;77(2):151-157.
32. Dewarrat F, Falco L, Caduff A, Talary M, Feldman Y, Puzenko A. Measurement and simulation of conductive dielectric two-layer materials with a multiple electrodes sensor. *IEEE Trans Dielectr Electr Insul*. 2008;15(5):1406-1414.
33. Talary M, Dewarrat F, Huber D, Caduff A. In vivo life sign application of dielectric spectroscopy and non invasive glucose monitoring. *J Non Cryst Solids*. 2007;353(47):4515-4517.
34. Caduff A, Talary M, Mueller M, et al. Non-invasive glucose monitoring in patients with type 1 diabetes: repeatability in the same subjects using a multisensor system. *Biosens Bioelectron*. 2009;24(9):2778-2784.
35. Forst T, Caduff A, Talary M, et al. Impact of environmental temperature on skin thickness and microvascular blood flow in subjects with and without diabetes. *Diabetes Technol Ther*. 2006;8:94-101.
36. Charkoudian N. Skin blood flow in adult human thermoregulation: how it works, when it does not, and why. *Mayo Clin Proc*. 2003;78(5):603-612.
37. Cobelli C, Ursino M. A model approach: mathematical modeling provides an increasingly clear picture of glucose and neural systems. *IEEE Pulse*. 2015;6(4):33-38.
38. Hastie T, Tibshirani R, Friedman JH. *The elements of statistical learning: data mining, inference, and prediction*. 2nd ed. Berlin, Germany: Springer; 2009.
39. Caduff A, Zanon M, Mueller M, et al. The effect of a global, subject, and device-specific model on a noninvasive glucose monitoring multisensor system. *J Diabetes Sci Technol*. 2015;9(4):865-872.
40. Zanon M, Sparacino G, Facchinetti A, et al. Non-invasive continuous glucose monitoring with multi-sensor systems: a Monte Carlo-based methodology for assessing calibration robustness. *Sensors (Basel)*. 2013;13(6):7279-7295.
41. Clarke WL, Cox D, Gonder-Frederick LA, Carter W, Pohl SL. Evaluating clinical accuracy of systems for self-monitoring of blood glucose. *Diabetes Care* 1987;10(5):622-628.
42. Clarke WL, Anderson S, Kovatchev B. Evaluating clinical accuracy of continuous glucose monitoring systems: continuous glucose-error grid analysis (CG-EGA). *Curr Diabetes Rev*. 2008;4(3):193-199.
43. Facchinetti A. Continuous glucose monitoring sensors: past, present and future algorithmic challenges. *Sensors (Basel)*. 2016;16(12). pii:E2093.
44. Guerra S, Sparacino G, Facchinetti A, Schiavon M, Man CD, Cobelli C. A dynamic risk measure from continuous glucose monitoring data. *Diabetes Technol Ther*. 2011;13(8):843-852.
45. Vettoretti M, Facchinetti A, Sparacino G, Cobelli C. Patient decision-making of CGM sensor driven insulin therapies in type 1 diabetes: In silico assessment. *Conf Proc IEEE Eng Med Biol Soc*. 2015;2015:2363-2366.
46. Pettus J, Price DA, Edelman SV. How patients with type 1 diabetes translate continuous glucose monitoring data into diabetes management decisions. *Endocr Pract*. 2015;(25):1-15.
47. Facchinetti A, Sparacino G, Cobelli C. Reconstruction of glucose in plasma from interstitial fluid continuous glucose monitoring data: role of sensor calibration. *J Diabetes Sci Technol*. 2007;1(5):617-623.
48. Lunn DJ, Wei C, Hovorka R. Fitting dynamic models with forcing function: application to continuous glucose monitoring in insulin therapy. *Stat Med*. 2011;30(18):2234-2250.